Journal of Molecular Structure 967 (2010) 131–139

Contents lists available at ScienceDirect

Journal of Molecular Structure

journal homepage: www.elsevier.com/locate/molstruc

Co-operation of π···π, Cu(II)···π, carbonyl···π and hydrogen-bonding forces leading to the formation of water cluster mimics observed in the reassessed crystal structure of [Cu(mal)(phen)(H_2O)]2·3H_2O (H_2mal = malonic acid, phen = 1,10-phenanthroline)

Somnath Ray Choudhury [a], Hon Man Lee [b], Tsun-Hung Hsiao [b], Enrique Colacio [c], Atish Dipankar Jana [d,*], Subrata Mukhopadhyay [a,*]

[a] Department of Chemistry, Jadavpur University, Kolkata 700 032, India
[b] Department of Chemistry, National Changhua University of Education, Changhua 50058, Taiwan
[c] Departamento de Química Inorgánica, Universidad de Granada, 18071-Granada, Spain
[d] Department of Physics, Sripat Singh College, Jiaganj, Murshidabad 742 123, India

ARTICLE INFO

Article history:
Received 4 September 2009
Received in revised form 23 December 2009
Accepted 31 December 2009
Available online 11 January 2010

Keywords:
Self-assembly
Crystal engineering
Molecular recognition
Carbonyl···π interaction
Copper(II) complex
1,10-Phenanthroline

ABSTRACT

A copper(II) malonate complex with formula [Cu(mal)(phen)(H_2O)]$_2$·3H_2O (**1**) [H_2mal = malonic acid, phen = 1,10-phenanthroline] has been synthesized and its crystal structure has been re-determined with an improved *R* value (the compound **1** was originally synthesized and crystallographically characterized by Kwik et al. with *R* = 0.047, see: J. Chem. Soc. Dalton Trans. (1986) 2529) with the water hydrogen atom positions located. This has led to the revelation that the water molecules organize around the carboxylate group of the malonate ligand forming tetramer, hexamer and octameric water cluster mimics. These cooperative hydrogen-bonding forces and various π-forces (π···π, Cu(II)···π, carbonyl···π) involving 1,10-phenanthroline aromatic rings determine the overall packing of the molecular units in the unit cell. There exists two identical monomers in the asymmetric unit with $Z^{/}$ = 2. TG measurements reveal the loss of water molecules that are all released at 120 °C. The water sorption/desorption process is reversible as supported by FTIR spectroscopic and XRPD studies.

1. Introduction

Quoting Dunitz, [1] a crystalline solid is a "supermolecule per excellence". Crystals nucleate and grow in the self-assembly process from molecular, atomic and sometimes even from soluble pre-formed 0D, 1D or 2D secondary building units. Our understanding regarding the self-assembly process at present is somewhat primitive which is reflected in Maddox's commentary that "one of the continuing scandals in physical sciences is the inability to predict a crystal structure even for the simplest of building blocks" [2,3]. The complicacies and sophistication of self-assembly process is due to the presence of various possible interactions which can lead to many ways of assembling the building blocks. Usually the strength of these possible interactions also come in a wide range including strong covalent force, intermediate coordinative force [4–7] and various weak forces such as hydrogen bonding [8–14], π···π interaction [15–30], C–H···π interaction [31,32], metal···π [33–38], anion···π interaction [39] and lone pair···π interaction [40–48]. The existence of phenomena like polymorphism [49–55] and high $Z^{/}$ or $Z^{//}$ crystal structures [56–60] are typical examples of this complexity (where $Z^{/} = Z/M$; *M* is the multiplicity of the general position and *Z* is the number of residues in the unit cell, $Z^{//}$ denotes the number of crystallographically non-equivalent molecules [60]). Even though we have some understanding how a set of molecular building blocks will mutually interact, sometimes the complexity of the self-assembly process is compounded even more due to the unpredictable inclusion of solvent molecules, especially water, that can drastically change the course of self-assembly. Under these circumstances to achieve the professed goal of crystal engineering – "the designed synthesis of crystals", one urgently needs to understand how various strong and weak forces can operate simultaneously in crystal packing – in other words how do these forces compete and/or cooperate? Although a knowledge-based approach [61] through data mining and analysis of structural databases such as CSD or ICSD seems to be the best way, sometimes a careful scrutiny of individual crystal structures can throw some light on the finer details and important principles of mutual cooperation and interaction of a number of strong and

* Corresponding authors. Tel.: +91 33 94331 63075; fax: +91 33 2414 6223.
E-mail addresses: atishdipankar@yahoo.com (A.D. Jana), smukhopadhyay@chemistry.jdvu.ac.in (S. Mukhopadhyay).

0022-2860/$ - see front matter © 2010 Elsevier B.V. All rights reserved.
doi:10.1016/j.molstruc.2009.12.048

weak forces operating simultaneously. In the present paper we report the re-determined [62] single-crystal X-ray structure of $[Cu(mal)(phen)(H_2O)]_2{\cdot}3H_2O$ (**1**) [mal = malonate dianion; phen = 1,10-phenanthroline] complex with improved *R* value (0.0263 as compared to 0.047 in [62]) and importantly with the water hydrogen atom positions determined from the difference Fourier map. This has helped us to unravel an important way in which the water molecules do cooperate among themselves and interact with the malonate ligands stabilizing the crystal packing crucially. Moreover, an in-depth analysis of the mode of operation of a number of weak forces (hydrogen bonding, π–π, metal–π and carbonyl–π) simultaneously occurring in the crystal structure has been carried out, which throws some light on the principle of cooperation of these forces. We show that relatively stronger hydrogen-bonding forces and comparatively weaker π-forces operate in a particular manner and the assemblies propagated by them are extended in mutually orthogonal direction. It is also shown that the weakest of the forces involved in the supramolecular assembly, namely, carbonyl–π and metal–π interactions are probably responsible for rendering the present solid-state structure into a class called "high $Z^{//}$ structures", which contains more than one identical molecular entity in the crystal asymmetric unit. Carbonyl···π interaction is a recent addition to the kitty of weak forces and the role it has played in the present crystal structure deserves attention. Another new revelation regarding this compound is its interesting reversible water sorption/desorption properties as evidenced by IR, TG and XRPD studies. This behavior is in consonance with the crystal structure and is possibly expected considering the fact that water molecules play important stabilizing roles in the crystal packing. Interestingly, compound **1** exhibits non-zero antiferromagnetic exchange interactions between the Cu(II) centers although these are part of monomeric complexes. The strong hydrogen bond interactions, as well as, the weak non-bonded metal–π, carbonyl–π and π–π interactions are responsible for these weak antiferromagnetic exchange interactions.

2. Experimental

2.1. Materials

Malonic acid, basic copper(II) carbonate and 1,10-phenanthroline were purchased from Sigma and used as received. Doubly distilled water was used throughout.

2.2. Synthesis of $[Cu(mal)(phen)(H_2O)]_2{\cdot}3H_2O$ (1)

Basic copper(II) carbonate, $CuCO_3{\cdot}Cu(OH)_2$, (0.221 g, 1 mmol) suspended in 20 mL of water was allowed to react with malonic acid (0.104 g, 1 mmol) at 50 °C to give a clear blue solution. Next, phenanthroline (0.180 g, 1 mmol) dissolved in 10 mL of methanol was added into the above solution at 50 °C under stirring. The resulting deep blue solution was heated at 50 °C for half an hour with continuous stirring. Then the solution was allowed to cool to room temperature and was left unperturbed for the slow evaporation of the solvent. Flat, deep blue, single crystals suitable for X-ray diffraction analysis appeared after 2 days. The crystals were filtered off, washed with cold water, and dried on filter paper. The yield was 65%. Anal. Calcd. for $C_{30}H_{30}N_4O_{13}Cu_2$: C, 46.10; H, 3.87; N, 7.17. Found: C, 45.85; H, 3.61; N, 6.89. This method of preparation is essentially the same as originally described [62] excepting that we used a different Cu(II) salt instead of $CuCl_2.2H_2O$ used by Kwik et al. [62] and the order of addition of the reagents differ.

2.3. Physical measurements

IR spectra of 1 were recorded on a Perkin–Elmer RXI FTIR spectrophotometer with the sample prepared as a KBr pellet in the range (4000–600 cm^{-1}). Elemental analyses (C, H, N) were performed on a Perkin–Elmer 240C elemental analyzer. Magnetization and variable-temperature (2–300 K) magnetic susceptibility measurements were carried out with a Quantum Design SQUID Magnetometer MPMS-XL at a static magnetic field of 0.5 T. Samples were fixed in gelatin capsules and held in drinking straws. Magnetization vs applied field measurements were carried out at 2.0 K in the field range of 0–5 T. Experimental data were corrected for the sample holder and for the diamagnetic contribution calculated from Pascal constants [63]. TGA analyses were carried out by using a Mettler Toledo TGA/SDTA 851^e system.

2.4. X-ray crystal structure determination

A single crystal having dimension $0.23 \times 0.23 \times 0.25$ mm^3 for **1** was used for data collection on an 'Bruker SMART APEX II' diffractometer equipped with graphite monochromated Mo Kα radiation ($\lambda = 0.71073$ Å) at 150 K. Theta range for data collection was 1.7–28.2°. A total of 15987 reflections were measured to give 7334 unique reflections ($R_{int} = 0.015$) for **1**. The 6567 data [$I > 2\sigma$] were used for solution and refinement by full-matrix least squares on F^2 using the SHELX-97 package [64]. The non-hydrogen atoms were refined anisotropically. The H atoms of the water molecules were located by difference Fourier map and their coordinates and thermal parameters were kept fixed. The other H atoms were treated by a riding model. The final *R* and R_w values are 0.0234 and 0.0660, respectively. Information concerning crystallographic data collection, refinement, bond length and angles, and supramolecular interactions are listed in Tables 1–5.

3. Results and discussion

3.1. Infrared spectroscopy

The absorption band at 3365 cm^{-1} (Fig. S1) can be assigned to the stretching vibration, υ(O–H), of the water molecules. υ_{as}(OCO) and υ_s(OCO) absorptions are observed at 1588 cm^{-1} and 1427 cm^{-1},

Table 1
Crystallographic data for compound **1**.

Compound	**1**
Formula	$C_{30}H_{30}N_4O_{13}Cu_2$
M	781.66
Crystal system	Triclinic
Space group	$P\bar{1}$ (No. 2)
a/Å	11.4644(6)
b/Å	11.6953(6)
c/Å	12.4544(6)
α (°)	92.041(2)
β (°)	105.502 (2)
γ (°)	110.007 (2)
F(0 0 0)	800
S(GOF)	1.07
V/Å^3	1497.06(13)
Z	2
T/K	150
Theta min–max (°)	1.7–28.2
ρ_{calc}/Mg m^{-3}	1.734
λ(Mo Kα)/Å	0.71073
μ(Mo Kα)/ mm^{-1}	1.50
Total reflections	15987
Unique data (R_{int})	7334 (0.015)
Observed data [$I > 2\sigma(I)$]	6567
Independent reflections [$I > 2\sigma(I)$]	7334
*R*1, $I > 2\sigma(I)$ (all)	0.0234
*wR*2, $I > 2\sigma(I)$ (all)	0.0660
Goodness of fit	1.07
Min. and max. resd. dens. (e/Å^3)	−0.48, 0.30

Table 2
Selected bond lengths (Å) and angles (deg) for **1**.

Cu(1)-O(1)	1.9287(12)	Cu(2)-N(4)	2.0258(12)
Cu(1)-O(2)	1.9097(10)	Cu(2)-O(7)	1.9046(13)
Cu(1)-O(5)	2.2458(11)	Cu(2)-O(10)	2.2724(12)
Cu(1)-N(1)	2.0160(13)	Cu(2)-O(6)	1.9303(10)
Cu(1)-N(2)	2.0233(13)	Cu(2)-N(3)	1.9920(14)
O(1)-C(13)	1.2784(19)	O(6)-C(30)	1.2743(19)
O(2)-C(15)	1.270(2)	O(7)-C(28)	1.2731(19)
O(3)-C(13)	1.2429(19)	O(8)-C(30)	1.2422(17)
O(4)-C(15)	1.2394(18)	O(9)-C(28)	1.240(2)
C(13)-C(14)	1.521(2)	C(28)-C(29)	1.514(2)
C(14)-C(15)	1.521(2)	C(29)-C(30)	1.519(2)
O(1)-Cu(1)-O(2)	94.65(5)	O(7)-Cu(2)-O(10)	95.92(5)
O(1)-Cu(1)-O(5)	93.53(5)	O(7)-Cu(2)-N(4)	90.61(5)
O(1)-Cu(1)-N(2)	92.64(5)	O(10)-Cu(2)-N(3)	85.97(5)
O(2)-Cu(1)-O(5)	98.94(5)	O(10)-Cu(2)-N(4)	94.48(5)
O(2)-Cu(1)-N(1)	89.01(5)	N(3)-Cu(2)-N(4)	81.96(5)
O(5)-Cu(1)-N(1)	96.37(5)	O(6)-Cu(2)-O(7)	94.39(5)
Cu(1)-O(1)-C(13)	128.12(9)	Cu(2)-O(6)-C(30)	126.39(10)
Cu(1)-O(2)-C(15)	129.61(10)	Cu(2)-O(7)-C(28)	127.32(11)
C(13)-C(14)-C(15)	122.71(14)	O(6)-Cu(2)-O(10)	100.51(4)
O(1)-C(13)-O(3)	121.93(13)	O(6)-Cu(2)-N(3)	92.43(5)
O(2)-C(15)-O(4)	121.81(14)	C(28)-C(29)-C(30)	119.22(12)
O(5)-Cu(1)-N(2)	93.97(5)	O(7)-C(28)-O(9)	121.91(14)
N(1)-Cu(1)-N(2)	81.46(5)	O(6)-C(30)-O(8)	122.60(14)

Table 3
Relevant H-bonds in compound **1**.

D–H···A	D–H (Å)	H···A (Å)	D···A (Å)	D–H···A (°)
O5–H5A···O3[a]	0.84	1.97	2.8014(18)	173
O5–H5B···O8	0.95	1.77	2.7075(16)	166
O10–H10A···O13[b]	0.92	1.85	2.757(2)	168
O10–H10B···O4	0.84	2.12	2.9313(17)	164
O11–H11A···O9	0.93	1.97	2.8882(19)	168
O11–H11B···O7[c]	0.89	2.60	3.3001(18)	137
O11–H11B···O9[c]	0.89	2.02	2.8908(17)	168
O12–H12A···O3	0.90	2.06	2.9536(17)	174
O12–H12B···O8[d]	0.87	1.96	2.8157(18)	168
O13–H13A···O11[b]	0.86	1.95	2.7976(19)	171
O13–H13B···O4[e]	0.86	1.91	2.7700(17)	176
C4–H4···O12[b]	0.95	2.41	3.236(2)	145
C7–H7···O9[f]	0.95	2.45	3.252(2)	142
C18–H18···O12[g]	0.95	2.42	3.2787(19)	149

[a] = 2 − *x*, 1 − *y*, 1 − *z*, [b] = 1 − *x*, 1 − *y*, 1 − *z*, [c] = 1 − *x*, 2 − *y*, − *z*, [d] = *x*, −1 + *y*, *z*, [e] = *x*, *y*, 1 + *z*, [f] = 1 − *x*, 2 − *y*, 1 − *z* and [g] = *x*, 1 + *y*, −1 + *z*.

Table 4
π–π interactions in **1**.

Cg(I)[a] → Cg(J)	Cg–Cg	Dihedral angle
Cg(3) → Cg(4)[i]	4.0234(9)	3.53
Cg(4) → Cg(12)[ii]	3.5525(9)	2.31
Cg(12) → Cg(12)[iii]	3.7688(9)	0.00

Symmetry code: (i) 1 − *x*, 1 − *y*, 1 − *z*; (ii) *x*, *y*, 1 + *z*; (iii) 2 − *x*, 2 − *y*, −*z*.
[a] Cg(I) denotes centroid of Ith ring; Ring (3) N(1)/C(1)/C(5)/C(4)/C(3)/C(2); Ring (4) N(2)/C(11)/C(10)/C(9)/C(8)/C(12); Ring (12) N(4)/C(16)/C(20)/C(19)/C(18)/C(17).

Table 5
Metal–π interactions in **1**.

Cg(I)[a] → Me(J)	Cg(I)–Me(J)
Cg(4) → Cu(1)[i]	3.87
Cg(5) → Cu(1)[i]	3.81
Cg(12) → Cu(2)[ii]	3.64

Symmetry code: (i) = 1 − *x*, 1 − *y*, 1 − *z*; (ii) = 2 − *x*, 2 − *y*, −*z*.
[a] Cg(I) denotes centroid of Ith ring; Ring (4) N(2)/C(11)/C(10)/C(9)/C(8)/C(12); Ring (5) C(1)/C(5)/C(6)/C(7)/C(8)/C(12); Ring (12) N(4)/C(16)/C(20)/C(19)/C(18)/C(17).

respectively. δ(OCO) absorptions are located at 790 and 724 cm^{-1}. The compound has been heated at 120 °C for 2 h under vacuum (0.1 mm Hg) in order to eliminate all the water molecules. Deliberate exposure to the laboratory atmosphere (34–36 °C, relative humidity 85–88%), such heated sample re-absorbed water molecules into the lattice as indicated by the IR spectrum (Fig. S2) when the re-appearance of the characteristic O–H stretching (3373 cm^{-1}) vibration is noticed. IR spectrum of **1** just after the heating could not be recorded because during the course of sample preparation and subsequent measurement, the heated sample started absorbing water, resulting in the observation of the characteristic O–H stretching vibration.

3.2. Thermal study

Thermogravimetric analyses (Figs. S3–S5) of compound **1** show that dehydration starts at about 65 °C and that all the lattice and coordinated water molecules are lost at 110 °C (calculated weight% for five lattice water molecules: 11.51%; found: 10.85%). The range of temperature to complete the dehydration suggests that the hydrogen-bonding association of the water molecules in the self-assembled structure is fairly strong. The complete decomposition of the dehydrated structure is achieved at ∼560 °C. Next, compound **1** has been heated for 2 h at 120 °C under 0.1 mm Hg pressure to completely remove all the water molecules prior to thermogravimetric analysis. The results show that water has been totally removed from the material since the corresponding loss step is not observed (Fig. S4). On deliberate exposure to ambient atmosphere for a few hours (34–36 °C, relative humidity 85–88%), the heated sample is capable of re-absorbing water which is evidenced by the emergence of the water loss steps in the TG curve (Fig. S5). The water desorption/sorption process is therefore fully reversible.

3.3. X-ray powder diffraction study

X-ray powder diffraction patterns (Figs. S6–S8) of compound **1** show major changes both in the peak positions and their intensities before and after water expulsion. Fig. S6 illustrates the XRD pattern of **1** at normal condition. The XRD pattern of **1** just after heating is depicted in Fig. S7, which shows the modifications of the peak positions and intensities (Figs. S6 and S7) arising from the complete removal of the water molecules. After cooling of the sample, its XRD pattern has been once more recorded which is comparable with that of the one obtained applying normal condition (Figs. S6 and S8). These XRPD study thus suggest that the cooled sample has re-absorbed water and that the process is reversible.

3.4. Description of the molecular structure of $[Cu(mal)(phen)(H_2O)]_2{\cdot}3H_2O$ (*1*)

The asymmetric unit consists of two crystallographically independent monomeric [Cu(mal)(phen)(H_2O)] units and three lattice water molecules. The ORTEP diagram of **1** is shown in Fig. 1. The coordination geometry around each copper(II) ions can be best described as a distorted square-pyramid with a CuN_2O_2O' chromophore. The τ value for Cu(1) is 0.07, while it is 0.15 for Cu(2). The structure index is defined as $\tau = (\beta - \alpha)/60$, where β and α are the largest coordination angles [65]. The Cu(1) and Cu(2) atoms reside 0.195(2) and 0.1523(2) Å above the basal plane, respectively, towards the coordinated water molecules. The basal plain for Cu1 unit is formed by the atoms N1/N2/O1/O2. The axial position is occupied by the oxygen atom O5 of a water molecule. The basal plane for Cu2 unit is completed by the atoms N3/N4/O6/O7. The axial position is occupied by the oxygen atom O10 of a water molecule. The angles subtended by the malonate ligands are 94.65°

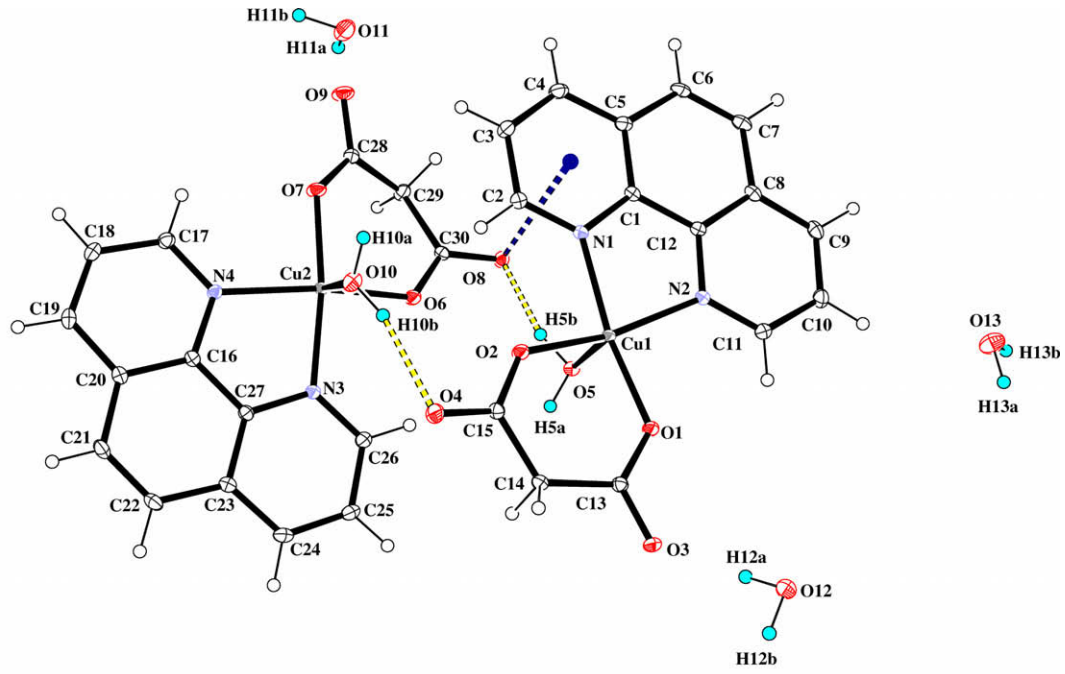

Fig. 1. ORTEP diagram of complex **1** at 50% ellipsoidal probability with atom numbering scheme. Presence of two identical units in the asymmetric unit ($Z^{/}$ = 2) and the formation of supramolecular dimer by these units should be noted.

and 94.39° for Cu1 and Cu2, respectively. No unusual bond lengths and bond angles are found for the chelated malonate ligand in **1** with respect to other malonate-containing copper(II) compounds [66]. The malonate moiety coordinated to the Cu(2) atom is more puckered than the one bond to the Cu(1) atom. The methylene carbon is more shifted than the chelate ring plane coordinated to Cu(2) compared to that of Cu(1).

The solid-state structure of compound **1** possesses a remarkable supramolecular architecture. Two monomeric [Cu(mal)(phen)-(H_2O)] units present in the asymmetric unit form a supramolecular dimer through strong complementary O10–H10B···O4 and O5–H5B···O8 hydrogen bonds assisted by weak carbonyl–π forces (Fig. 2). The hydrogen bonded supramolecular dimer (Fig. 2) is additionally stabilized by the recently recognized novel carbonyl–π interaction [40–48]. Here it operates between the carboxylate C(30)═O(8) group of the malonato ligand bound to Cu(2) and the π system of the ring N1/C1/C5/C4/C3/C2 belonging to the phenanthroline ligand coordinated to Cu(1) (Fig. 2).

Uncoordinated carboxylate oxygen atom O8 [which is also involved in strong H bonding with water molecule, O5–H5B···O8 = 2.7075(16) Å] is interacting with the pyridyl ring of the phenanthroline ligand [C(30)–O(8)···Cg(3) = 3.3249(14) Å and the angle C(30)–O(8)–Cg(3) is 93.43(9)°; Cg(3) is the centroid of the ring defined by the atoms N1/C1/C5/C4/C3/C2]. The shortest separation distance between the carbonyl group and the ring carbon atoms that reflects this interaction as C30···C2 = 3.148(2) Å, which is below the sum of the corresponding van der Waals radii [67]. A recent analysis of the Cambridge Structural Database (CSD) for lone pair···π interactions by Egli et al. [41] has shown that a strong carbonyl (π) – π (aromatic) stacking interaction is suggested by an angle ω ranging from 0° to 24°, ω being the dihedral angle between the C═O bond and the plane of the aromatic ring. In **1**, the orientation of the carbonyl group is not parallel to the ring ($\omega \approx 15.47°$), and is therefore indicative of a significant carbonyl (π) – π (aromatic) stacking interaction. As stated by Egli et al. [41], this orientation potentially allows hydrogen bonding interactions with the

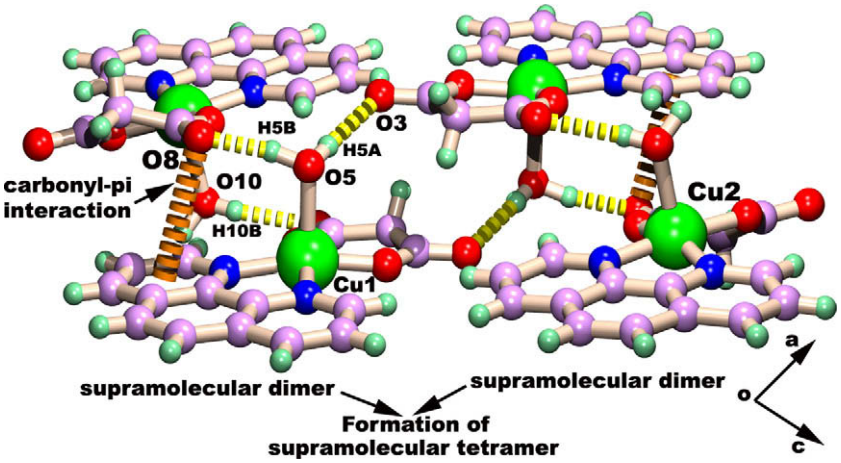

Fig. 2. Carbonyl···π contact within supramolecular dimer and the formation of supramolecular tetramer.

oxygen lone pairs. A hydrogen bond is indeed observed for O8 which interacts with the oxygen atom O5 of a neighboring Cu(1) unit (O5–H5B···O8 = 2.7075(16) Å; Table 3). Moreover, the distance *D* (corresponding to the distance between the carbonyl oxygen atom and the ring centroid) and the angular distribution [deviation of the angle α (α is the angle >C=O–Cg) from 120°] are 3.32 Å and 26.57°, respectively. These values are within the mean values, *i.e.* 3.58 and 30.6°, calculated by Egli et al. [9b], Hence in **1**, significant carbonyl (π) – π (aromatic) stacking interaction exists and due to its recent recognition, was naturally overlooked in the previous and first report of **1** [62]. However, we have unraveled an interesting scenario in which the strong hydrogen bonding force [O5–H5B···O8 and O10–H10B···O4] and weak carbonyl–π force can act in unison cooperating with each other although they operate in nearly orthogonal direction.

These supramolecular dimers, due to their inherent self-complementarity, form supramolecular tetramers through the O5–H5A···O3 hydrogen bonds (Fig. 2). These tetrameric units can be considered as repeating units that generate the extended supramolecular layer structure (Fig. 3) present in **1**.

The organization of these tetrameric units, producing a 2D supramolecular sheet (Fig. 3), is achieved though the participation of three lattice water molecules [O11(H11A, H11B); O12(H12A, H12B); O13(H13A, H13B)] that act as stabilizing agents by saturating the uncoordinated malonate oxygen atoms through hydrogen bonding interactions (Table 3). It is to be noted that these lattice water molecules arrange in such a way that they produce water cluster mimics – actually, structures analogous to those of planar water tetramer [68], chair form water hexamer [69–77] and ring-shaped water octamer [78] are formed. In these cluster mimics, uncoordinated malonate O atoms of two symmetry related counterparts have replaced two water molecules in each of the above mentioned free water clusters motifs. The water oxygen atom O11(H11A, H11B) and the malonate oxygen atom O9 generate the tetramer analogue with an average O···O distance of 2.89 Å. This distance is close to that predicted from laser spectroscopic (vibration–rotation–tunneling, VRT) experiment for a regular gas phase tetramer water cluster (2.79 Å) [79]. In the formation of the water hexamer mimic, one coordinated water molecule [O10(H10A, H10B)], one lattice water molecule [O13(H13A, H13B)] and the oxygen atom O4 from a malonate are involved. Whereas the coordinated O10 atom acts as double donor and the malonate O4 atom behaves as double acceptor, the lattice water molecule O13 acts as both single donor and single acceptor within the water hexamer cluster mimic. The average O···O distance in the hexamer mimic is 2.82 Å, which is close to the distance found in liquid water (2.85 Å) [80]. The corresponding value is 2.759 Å in ice I_h at −90 °C [81]. The bond angles in the hexamer mimic vary widely with the average angle being 107.71°, which is interestingly very close to the corresponding value of 109.3° found in hexagonal ice. Hence, the average O···O distances and angles found in this mimic are similar to those of a regular hexagonal water cluster in chair conformation [69–77]. The fact that the cluster mimic is structurally close to a regular water cluster although it is generated by the simultaneous participation of coordinated water molecules and malonate O atoms is interesting. Indeed, this feature suggests that the clustering tendency of water molecules probably has some structure-assembling influence in the supramolecular self-assembly. Regular octamer water clusters have been found in various three-dimensional topologies [82–86,71,87,88], but the ring-form water cluster has been first observed in a crystalline host [78]. The stability of the ring-form water octamer has been subsequently established through *ab initio* computational studies [82,89–95]. The present octamer cluster mimic is generated from one coordinated water molecule O12(H12A,H12B), one lattice water molecule O5(H5A,H5B), two malonate O atoms (O8 from the Cu2 unit and O3 from the Cu1 unit) and their symmetry related counterparts. The average O···O distance in this case is 2.82 Å.

The supramolecular sheet achieved through the simultaneous formation of tetramer, hexamer and octamer water mimics is found in the $(\bar{1}\,0\,2)$ crystal plane. The particular arrangement in this plane can be further visualized as the integration of ribbons running parallel to each other and joined at their edges through the octamer mimics (Fig. 3). At the center of each ribbon runs

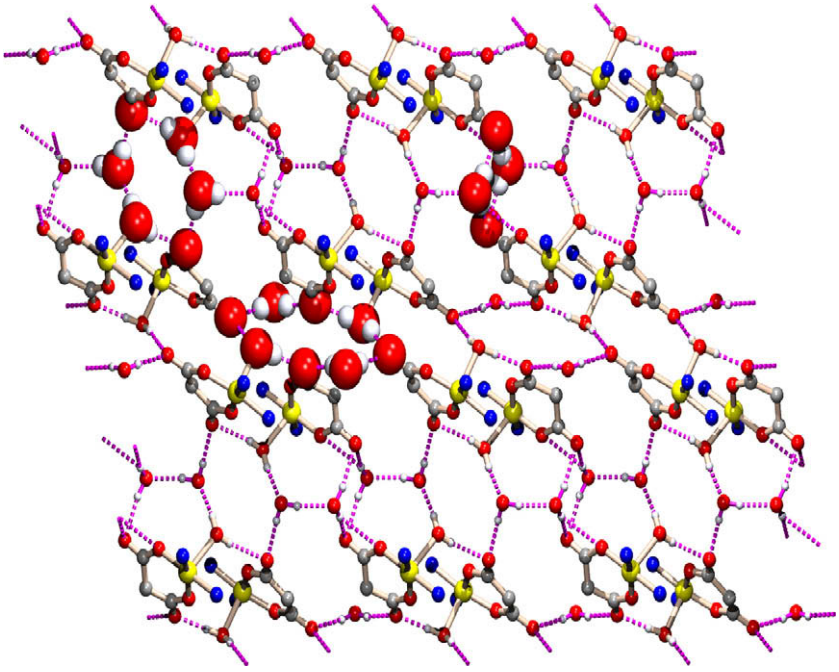

Fig. 3. Assembly of supramolecular dimers through water–oxygen (malonate) cluster motifs that mimic water tetramer, hexamer and octamer (phenanthroline ligands are omitted for the clarity of the picture).

the polymeric chain of successive tetramer and hexamer water mimics (Fig. 4), along the crystallographic *b*-axis.

Phenanthroline ligands on this plane are organized in such a way that it protrude out on both sides (Fig. S9), facilitating the packing of successive sheets through π–π, metal–π and carbonyl–π interactions. Cooperation of these π forces has been depicted in Fig. 5.

As can be seen from Fig. 5, adjacent Cu1 centers interact among themselves through π···π (4.02 Å) and Cu(II)···π (3.87 and 3.81 Å) (Tables 4 and 5). These forces generate a dimeric unit comprising of two Cu1 units. Carbonyl···π interactions (3.69 and 3.64 Å) join Cu2 units on either side of the above-mentioned dimeric units of Cu1, thus generating a tetrameric unit comprising two Cu2 units and two Cu1 units. Successive Cu2 units are joined by π···π (3.77 Å) and Cu2···π (3.64 Å) interaction. The appearance of two crystallographic non-equivalent Cu centers (Cu1 and Cu2) can be assigned to the two carbonyl···π interactions between successive Cu1 and Cu2 centers. It has to be noted that whereas the hydrogen bonding interactions lead to the organization of the monomeric units into a planar sheet structure, relatively weaker π-interaction forces operate to extend the supramolecular assembly in a perpendicular direction. This mode of operation of strong hydrogen-bonding forces and weak π–π forces has been recently utilized by us to engineer layered crystalline materials [96] and has been observed in a number of other cases [97–99]. The important point to be noted is the non-interfering nature of weak and strong forces present simultaneously in a competitive environment.

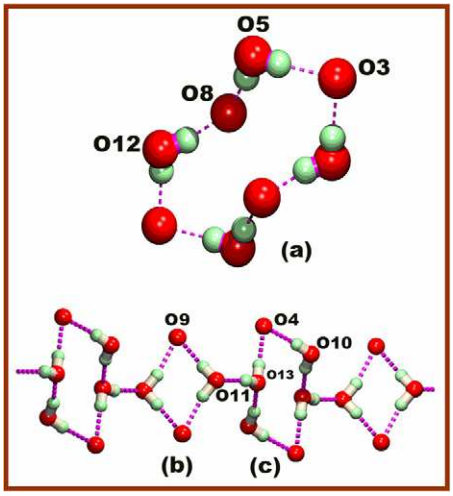

Fig. 4. Water cluster mimics, octamer (a), tetramer (b), and hexamer (c), in which some of the water molecules have been replaced by malonate oxygen atoms.

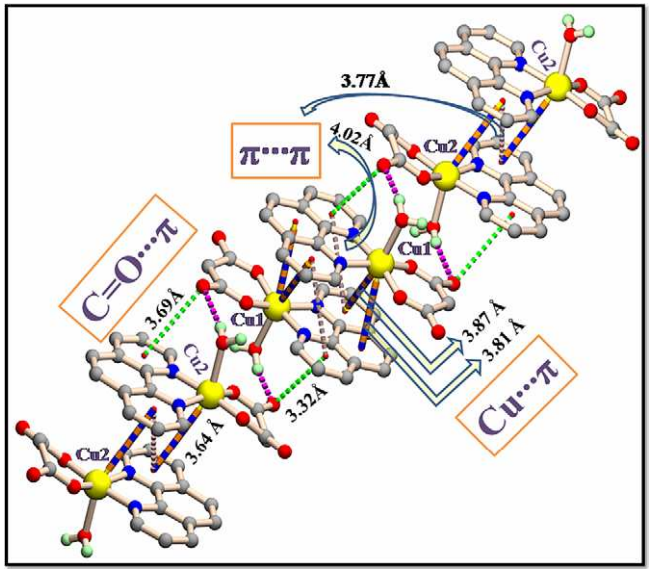

Fig. 5. π···π, Cu(II)···π and carbonyl···π interactions among successive Cu1 and Cu2 centers generating two crystallographically non-equivalent Cu centers ($Z^{//} = 2$).

3.5. Magnetic study

The magnetic properties of **1** in the form of a $\chi_M T$ vs T plot [χ_M being the molar susceptibility per copper(II) ion] are shown in Fig. 6. $\chi_M T$ at room temperature is 0.413 $cm^3\ mol^{-1}$ K, which is an expected value for a magnetically isolated spin doublet with $g = 2.10$, and remains almost constant down to 10 K. Below this temperature, the $\chi_M T$ product decreases sharply to reach a value of 0.36 $cm^3\ mol^{-1}$ K at 2 K. This behaviour is consistent with the presence of a very weak antiferromagnetic interaction between the Cu(II) atoms. The susceptibility data follow the Curie–Weiss law with a Weiss constant θ value of −0.08 K. The Weiss constant can be used to estimate the value of the interaction by using the mean-field expression: $\theta = zJS(S+1)/3k$, where z is the number of nearest neighbours, J is the exchange coupling constant, S is the spin and k the Boltzmann constant. The estimated value is $zJ = -0.21\ cm^{-1}$.

Three magnetic exchange pathways can mainly operative in this compound: (i) strong hydrogen bond interactions involving the coordinated water molecule and axial position and one of the oxygen atoms of the malonate ligand belonging to a neighbouring molecule (Cu–Ow–O–C–O–Cu) (ii) strong hydrogen bond interactions involving the coordinated water molecule, one non-coordinated water molecules and the malonate ligand from another neighbouring molecule (Cu–Ow–Ow–O–C–O–Cu) (iii) the π–π interactions between phenantroline rings and (iv) the carbonyl–π interaction and metal–π interactions. All these magnetic exchange pathways are known to be very poor in mediating magnetic exchange couplings, which is consistent with the very small J value observed for **1**. Among the magnetic exchange pathways, the σ ones (i) and (ii) are probably the more efficient in mediating the magnetic coupling. Because (i) is shorter that (ii), the former must be the main contribution to the observed J value.

3.6. Discussion on the crystal structure of *1*

The formation of coordination or supramolecular architectures obviously depends on the choice of the set of building blocks.

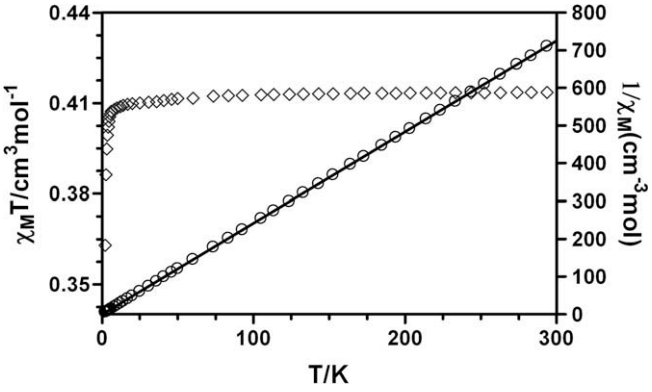

Fig. 6. Temperature dependence of $\chi_M T$ (squares) and $1/\chi_M$ vs T (circles) for **1**. The solid line represents the fit of experimental data to the Curie–Weiss equation in the form $1/\chi_M = (T-\theta)/C$.

Transition or rare-earth metals are generally used in the design of metal–organic frameworks in which they act as nodes in the network propagated by various bridging ligands (usually organic species) or by supramolecular links. Due to the inherent information encoding capability through their preferred coordination geometries, these metal atoms like the bridging ligands also, determine the architecture of the network. Depending upon the ligand environment, transition metals including Cu(II) show many preferred coordination geometries. For the successful prediction of a crystal structure which is one of the stated goals of crystal engineering, a clear understanding of the conditions in which a targeted coordination environment is achieved is essential. For instance, five-coordinate copper complexes may adopt a square-pyramidal or a trigonal–bipyramidal coordination geometry. The choice of the ligands and the physico-chemical conditions in which the coordination materials are synthesized are undoubtedly playing a role in the generation of the two different environments. In the present case, the malonate ligand exhibits both chelating and bridging capabilities while phenanthroline has only chelating abilities. A retrospective analysis of the packing arrangements allows establishing the conditions under which the copper ion prefers a square-pyramidal coordination environment. Due to relatively larger size of phenanthroline compared to malonate, no coordination network through the bridging capability of malonate is possible; instead, the malonate unit prefers to chelate the metal center which most likely facilitates the formation of dimeric hydrogen-bonded square-pyramidal copper(II) entity having an axially coordinated water molecule. The influence of the choice of the reaction medium is evident from the crucial role played by the water molecules in the supramolecular network herein described. The hydrogen-bonding association of the malonate ligands with water molecules gives rise to a 2D supramolecular sheet. It is interesting to notice that the water molecules and the malonate oxygen atoms form distinct supramolecular motifs. These motifs can be regarded as mimics of regular water clusters such as the tetramer, the hexamer and the octamer cluster in which some of the water molecules are replaced by O atoms from malonate units. Even with the intrusion of the water molecules in the tetramer mimic, the average O···O distance is 2.89 Å, close to the one found in the gas phase tetramer. [79] Generally, water hexamers have been found in various nearly isoenergic forms like chair, boat, prism, cage, book and bag [100–107]. In the present chair form water hexamer mimic, the average O···O distance is 2.82 Å – close to 2.85 Å which has been found in the liquid phase [80]. Water octamers usually are found in the cubic S_4 or D_{2d} form [101,102,108,109] or in the open-cubic form [84,110]. In the ring-form water octamer mimic found here, the average O···O distance is 2.82 Å and that found in *ab initio* calculation is 2.71 Å. [105]. Moreover, in these motifs, the water molecules include lattice water molecules as well as coordinated water molecules. The fact that even with the participation of coordinated water molecules the different molecular arrangements try to reach the regular water cluster geometries indicates that, in the overall supramolecular assembly, the clustering tendency of the water molecules is an important issue. Another point to be noted is that the dimeric units and the water molecules organize to form a supramolecular sheet in such a way that each supramolecular motif and the dimer of dimer have a centrosymmetric arrangement. Centric arrangements generally arise to quell the imbalance in dipole moment and may be assumed to be a phenomenon guiding the organization of water molecules into clusters [111]. Most of the water molecules in the present structure are involved in tri-directional interactions which is in agreement with the inferred tendency of water molecules as shown by a CSD database analysis [112]. The phenanthroline ligands due to their π-electronic abundance tend to take part in π-stacking interactions and the organization of the phenanthrolines in the supramolecular sheet is reflected by this feature. As a result, the phenanthroline units are aligned outwards of the water/malonate mean plane, on both sides, which is also the reason why the basic unit in the structure is a centrosymmetic dimer. This type of arrangement into a planar sheet is a common phenomenon generally observed when a combination of at least two ligands is used, one of them having hydrogen bonding abilities (like dicarboxylates) and the other having π-interaction capabilities (such as bipyridine and phenanthroline). As expected, the sheets stack through π–π interaction forming a 3D supramolecular assembly. The importance of π–π interaction in crystal engineering has long been recognized [25,26] and these have been explored theoretically also [27–30] but the relatively weaker metal–π and carbonyl–π interactions has been paid little attention that needs further theoretical study. A subtle effect of these weak forces seems to be responsible for the high Z' ($Z' = 2$) nature, *i.e.* more than one identical units are found in the asymmetric unit (Fig. 1) of the complex. The appearance of high Z' or Z' complexes is an intriguing phenomenon, often thought of as 'relic fossils' or 'crystal on the way' [56–60] and weak forces are believed to be responsible for the appearance of such rare crystals. Among the two Cu centers (Cu1 and Cu2) in the asymmetric unit of the present complex, π–π and metal–π interactions are involved in uniting Cu1···Cu1 centers but carbonyl–π, π–π and metal–π interactions are responsible in uniting Cu1···Cu2 centers while the other one is solely involved in π–π interactions. In the present complex the appearance of multiple non-equivalent Cu units can probably be assigned to the asymmetric nature of the cooperation of these weak forces.

4. Conclusions

In sum, the single-crystal X-ray structure of a coordination compound, namely $Cu(mal)(phen)(H_2O)]_2{\cdot}3H_2O$ (**1**), has been redetermined and some important structural points regarding the role of weak forces in the crystal lattice are emphasized. The determination of the exact positions of the hydrogen atoms from the water molecules reveals that these water molecules tend to retain their regular vapor-phase geometries in the solid-state structure of **1** *albeit* with the participation of donor oxygen atoms from dicarboxylate ligands. It appears that these water arrangements aid the stabilization of the supramolecular architecture. Furthermore, compound **1** has reversible water sorption/desorption properties which most likely arise from the hydrogen-bonding association between the water molecules and the organic moieties observed in its crystal lattice. Finally, the role played by weak forces, especially carbonyl–π and metal–π interactions, appear to be crucial as they are most likely behind the presence of multiple crystallographically non-equivalent identical entities in the asymmetric unit – a phenomenon meagerly understood but potentially important for crystal structure prediction. The present crystal structure, though a case study, corroborates the general belief that the origin of high Z' structures lies in the mutually cooperative nature of weak forces like the ones found here.

Acknowledgements

S.M. is grateful to UGC-CAS programme in the Department of Chemistry, Jadavpur University for financial support of this work. H.M.L. is grateful to the National Science Council of Taiwan for financial support of this work. E.C. acknowledges the MEC (Spain) (Project CTQ2005/0935) and the Junta de Andalucía (FQM-195) for financial support.

Appendix A. Supplementary data

Full crystallographic data in CIF format for **1** have been deposited with the Cambridge Crystallographic Data Centre (CCDC No. 718065). Copies of the data can be obtained, free of charge, on application to CCDC, 12 Union Road, Cambridge, CB2 1EZ, U.K; Fax: +44(0)-1223-336033; or email: deposit@ccdc.cam.ac.uk. Supplementary data associated with this article can be found, in the online version, at doi:10.1016/j.molstruc.2009.12.048.

References

[1] J.D. Dunitz, In: G.R. Desiraju (Ed.), Perspectives in Supramolecular Chemistry: The Crystal as a Supramolecular Entity, vol. 2, Wiley, Chichester, 1996 (Chapter 1).
[2] J. Maddox, Nature 335 (1988) 201.
[3] S.L. Price, Acc. Chem. Res. 42 (2009) 117.
[4] L. Pauling, The Nature of the Chemical Bond, Cornell University Press, Ithaca, NY, 1939.
[5] W.A. Goddard, Nature of the Chemical Bond III, California Institute of Technology, Pasadena, CA, 1986.
[6] F.A. Cotton, G. Wilkinson, P.L. Gaus (Eds.), Basic Inorganic Chemistry third ed, John Wiley and Sons Inc., 1994.
[7] C. Housecroft, A.G. Sharpe (Eds.), Inorganic Chemistry, second ed, Prentice Hall, 2004.
[8] G.R. Desiraju, T. Steiner (Eds.), The Weak Hydrogen Bond in Structural Chemistry and Biology, Oxford University Press, Oxford, 1999.
[9] G.A. Jeffrey, W. Saenger (Eds.), Hydrogen Bonding in Biological Structures, Springer, Berlin, 1991.
[10] W.C. Hamilton, J.A. Ibers (Eds.), Hydrogen Bonding in Solids, Benjamin, New York, 1968.
[11] S. Scheiner, Hydrogen Bonding: A Theoretical Perspective, Oxford University Press, Oxford, 1997.
[12] G.A. Jeffrey, An Introduction to Hydrogen Bonding, Oxford University Press, Oxford, 1997.
[13] T. Steiner, Angew. Chem. Int. Ed. 41 (2002) 48.
[14] S.-I. Noro, T. Akutagawa, T. Nakamura, Cryst. Growth Des. 7 (2007) 1205.
[15] C. Janiak, J. Chem. Soc., Dalton Trans. (2000) 3885.
[16] O. Yamauchi, A. Odani, S. Hirota, Bull. Chem. Soc. Jpn. 74 (2001) 1525.
[17] M.J. Packer, M.P. Dauncey, C.A. Hunter, J. Mol. Biol. 295 (2000) 71.
[18] M.J. Packer, M.P. Dauncey, C.A. Hunter, J. Mol. Biol. 295 (2000) 85.
[19] K. Müller-Dethlefs, P. Hobza, Chem. Rev. 100 (2000) 143.
[20] R. Ghosh, A.D. Jana, S. Pal, G. Mostafa, H.-K. Fun, B.K. Ghosh, CrystEngComm 9 (2007) 353.
[21] S.R. Choudhury, J. Bhattacharyya, S. Das, B. Dey, S. Mukhopadhyay, L.-P. Lu, M.-L. Zhu, Acta Crystallogr E63 (2007) m1331.
[22] B.L. Schottel, H.T. Chifotides, M. Shatruk, A. Chouai, L.M. Pérez, J. Bacsa, K.R. Dunbar, J. Am. Chem. Soc. 128 (2006) 5895.
[23] A.D. Jana, A.K. Ghosh, D. Ghoshal, G. Mostafa, N.R. Chaudhuri, CrystEngComm 9 (2007) 304.
[24] A.D. Jana, S.C. Manna, G.M. Rosair, M.G.B. Drew, G. Mostafa, N.R. Chaudhuri, Cryst. Growth Des. 7 (2007) 1365.
[25] P. Hobza, H.L. Selzle, E.W. Schlag, Chem. Rev. 94 (1994) 1767.
[26] K.S. Kim, P. Tarakeshwar, J.Y. Lee, Chem. Rev. 100 (2000) 4145.
[27] M.O. Sinnokrot, C.D. Sherrill, J. Phys. Chem. A 110 (2006) 10656.
[28] E.C. Lee, D. Kim, P. Jurecka, P. Tarakeshwar, P. Hobza, K.S. Kim, J. Phys. Chem. A 111 (2007) 3446.
[29] M. Pitonak, P. Neogrady, J. Rezac, P. Jurecka, M. Urban, P. Hobza, J. Chem. Theory Comput. 4 (2008) 1829.
[30] N.J. Singh, S.K. Min, D.Y. Kim, K.S. Kim, J. Chem. Theory Comput. 5 (2009) 515.
[31] M. Nishio, CrystEngComm 6 (2004) 130 (and references therein).
[32] M. del, C. Fernandez-Alonso, F.J. Canada, J. Jimenez-Barbero, G. Cuevas, J. Am. Chem. Soc. 127 (2005) 7379.
[33] A.K. Ghosh, D. Ghosal, J. Ribas, G. Mostafa, N.R. Chaudhuri, Cryst. Growth Des. 6 (2006) 36.
[34] A. Vigalok, D. Milstein, Acc. Chem. Res. 34 (2001) 798.
[35] T. Probst, O. Steigelmann, H. Riede, H. Schmidbaur, Chem. Ber. 124 (1991) 1089.
[36] H. Schmidbaur, W. Bublak, B. Huber, G. Müller, Angew. Chem. Int. Ed. Engl. 26 (1987) 234.
[37] H. Schmidbaur, R. Nowak, O. Steigelmann, G. Müller, Chem. Ber. 123 (1990) 1221.
[38] W.J. Vickaryous, R. Herges, D.W. Johnson, Angew. Chem. Int. Ed. Engl. 43 (2004) 5831.
[39] P. Gamez, T.J. Mooibroek, S.J. Teat, J. Reedijk, Acc. Chem. Res. 40 (2007) 435.
[40] M. Egli, R.V. Gessner, Proc. Natl. Acad. Sci. USA 92 (1995) 180.
[41] M. Egli, S. Sarkhel, Acc. Chem. Res. 40 (2007) 197.
[42] J.E. Gautrot, P. Hodge, D. Cupertinob, M. Helliwell, New J. Chem. 30 (2006) 1801.
[43] T.J. Mooibroek, S.J. Teat, C. Massera, P. Gamez, J. Reedijk, Cryst. Growth Des. 6 (2006) 1569.
[44] R.J. Santos-Contreras, F.J. Martínez-Martínez, E.V. García-Báez, I.I. Padilla-Martínez, A.L. Peraza, H. Höpfl, Acta Crystallogr C63 (2007) o239.
[45] Z. Lu, P. Gamez, I. Mutikainen, U. Turpeinen, J. Reedijk, Cryst. Growth Des. 7 (2007) 1669.
[46] C.-Q. Wan, X.-D. Chen, T.C.W. Mak, CrystEngComm 10 (2008) 475.
[47] S.R. Choudhury, P. Gamez, A. Robertazzi, C.-Y. Chen, H.M. Lee, S. Mukhopadhyay, Cryst. Growth Des. 8 (2008) 3773.
[48] S.R. Choudhury, B. Dey, S. Das, P. Gamez, A. Robertazzi, K.-T. Chan, H.M. Lee, S. Mukhopadhyay, J. Phys. Chem. A 113 (2009) 1623.
[49] Y. Sonoda, F. Hirayama, H. Arima, Y. Yamaguchi, W. Saengerb, K. Uekama, Chem. Commun. (2006) 517.
[50] J.S. Tse, D.D. Klug, J. Ripmeester, A.S. Desgreniers, K.L. Lagarec, Nature 369 (1994) 724.
[51] J. Bernstein, Polymorphism in Molecular Crystals, Oxford University Press, Oxford, 2002.
[52] P. Munshi, T.N. Guru Row, Cryst. Growth Des. 6 (2006) 708.
[53] J.M. Zhang, D.J. Njus, C. Sandman, B.M. Guo, P.E. Foxman, R. Gelder, Chem. Commun. (2004) 886.
[54] L. Fabian, A. Kalman, G. Argay, G. Bernath, Z.C. Gyarmati, Chem. Commun. (2004) 2114.
[55] T.V. Timofeeva, Kinnibrugh, O.Ya. Borbulevych, B.B. Averkiev, V.N. Nesterov, A. Sloan, M.Y. Antipin, Cryst. Growth Des. 4 (2004) 1265.
[56] D. Das, R. Banerjee, R. Mondal, J.A.K. Howard, R. Boese, G.R. Desiraju, Chem. Commun. (2006) 555.
[57] S.K. Chandran, A. Nangia, CrystEngComm 8 (2006) 581.
[58] G.R. Desiraju, CrystEngComm 9 (2007) 91.
[59] K.M. Anderson, J.W. Steed, CrystEngComm 9 (2007) 328.
[60] B.P. van Eijck, J. Kroon, Acta Cryst. B56 (2000) 535 (erratum: ibid, 745).
[61] J. Chisholm, Pidcock, J.v. de Streek, L. Infantes, S. Motherwell, F.H. Allen, CrystEngComm 8 (2006) 11.
[62] W.-L. Kwik, K.-P. Ang, H.S.-O. Chan, V. Chebolu, S.A. Koch, J. Chem. Soc. Dalton Trans. (1986) 2519 (and references cited therein).
[63] E.A. Boudreaux, L.N. Mulay, Theory and Applications of Molecular Paramagnetism, John Wiley and Sons, New York, 1976.
[64] G.M. Sheldrick, SHELXL97: Program for the Refinement of Crystal Structures, University of Göttingen, Göttingen, Germany, 1997.
[65] A.W. Addison, T.N. Rao, J. Reedijk, J.V. Rijn, G.C. Verschoor, J. Chem. Soc. Dalton Trans. 7 (1984) 1349.
[66] J. Pasán, J. Sanchiz, F. Lloret, M. Julve, C. Ruiz-Pérez, CrystEngComm 9 (2007) 478 (and references cited therein).
[67] A. Bondi, J. Phys. Chem. 68 (1964) 441.
[68] O. Fabelo, J. Pasán, L. Cañadillas-Delgado, F.S. Delgado, A. Labrador, F. Lloret, M. Julve, C. Ruiz-Pérez, CrystEngComm 10 (2008) 1743 (and references therein).
[69] R. Custalcean, C. Afloroaiei, M. Balsa, M. Polverejan, Angew. Chem. Int. Ed. 39 (2000) 3094.
[70] X.-M. Zhang, R.-Q. Fang, H.-S. Wu, Cryst. Growth Des. 5 (2005) 1335.
[71] B.-Q. Ma, H.-L. Sun, S. Gao, Chem. Commun. (2005) 2336.
[72] B.-H. Ye, B.-B. Ding, Y.-Q. Weng, X.-M. Chen, Inorg. Chem. 43 (2004) 6866.
[73] S.K. Ghosh, P.K. Bharadwaj, Inorg. Chem. 42 (2003) 8250.
[74] J.N. Moorthy, R. Natarajan, P. Venugopalan, Angew. Chem. Int. Ed. 41 (2002) 3417.
[75] K.-M. Park, R. Kuroda, T. Iwamoto, Angew. Chem. Int. Ed. Engl. 32 (1993) 884.
[76] U. Mukhopadhyay, I. Bernal, Cryst. Growth Des. 5 (2005) 1687.
[77] Y.-C. Liao, Y.-C. Jiang, Am. Chem. Soc. 127 (2005) 12794.
[78] J.L. Atwood, L.J. Barbour, T.J. Ness, C.L. Raston, P.L. Raston, J. Am. Chem. Soc. 123 (2001) 7192.
[79] J.D. Cruzan, L.B. Braly, K. Liu, M.G. Brown, J.G. Loeser, R.J. Saykally, Science 271 (1996) 59.
[80] A.H. Narten, W.E. Thiessen, L. Blum, Science 217 (1982) 1033.
[81] D. Eisenberg, W. Kauzmann, The Structure and Properties of Water, Oxford University Press, Oxford, 1969.
[82] R. Ludwig, Angew. Chem. Int. Ed. 40 (2001) 1808.
[83] D. Li, Y. Wang, X. Luan, P. Liu, C. Zhou, H. Ma, Q. Shi, Eur. J. Inorg. Chem. (2005) 2678.
[84] R.J. Doedens, E. Yohannes, M.I. Khan, Chem. Commun. (2002) 62.
[85] W.B. Blanton, S.W. Gordon-Wylie, G.R. Clark, K.D. Jordan, J.T. Wood, U. Geiser, T.J. Collins, J. Am. Chem. Soc. 121 (1999) 3551.
[86] S. Kar, B. Sarkar, S. Ghumaan, D. Janardanan, J. van Slageren, J. Fiedler, V.G. Puranik, R.B. Sunoj, W. Kaim, G.K. Lahiri, Chem. Eur. J. 11 (2005) 4901.
[87] T.K. Prasad, M.V. Rajasekharan, Cryst. Growth Des. 6 (2006) 488.
[88] M.V. López, G. Zaragoza, M. Otero, R. Pedrido, G. Rama, M.R. Bermejo, Cryst. Growth Des. 8 (2008) 2083.
[89] S. Maheshwary, N. Patel, N. Sathyamurthy, A.D. Kulkarni, S.R. Gadre, J. Phys. Chem. A 105 (2001) 10525.
[90] C. Lee, H. Chen, G. Fitzgerald, J. Chem. Phys. 102 (1995) 1266.
[91] C.J. Tsai, K.D. Jordan, J. Phys. Chem. 97 (1993) 5208.
[92] K. Laasonen, M. Parrinello, R. Car, C. Lee, D. Vanderbilt, Chem. Phys. Lett. 207 (1993) 208.
[93] C.J. Tsai, K.D. Jordan, J. Chem. Phys. 95 (1991) 3850.
[94] C.J. Tsai, K.D. Jordan, J. Chem. Phys. 99 (1993) 6957.
[95] S. Maeda, K. Ohno, J. Phys. Chem. A 111 (2007) 4527.
[96] B. Dey, S.R. Choudhury, E. Suresh, A.D. Jana, S. Mukhopadhyay, J. Mol. Struct. 921 (2009) 268.
[97] R. Ghosh, A.D. Jana, S. Pal, G. Mostafa, H.-K. Fun, B.K. Ghosh, CrystEngComm 9 (2007) 353 (and references therein).

[98] A.D. Jana, A.K. Ghosh, D. Ghoshal, G. Mostafa, N. Ray Chaudhuri, CrystEngComm 9 (2007) 304 (and references therein).
[99] A.D. Jana, S.C. Manna, G.M. Rosair, M.G.B. Drew, G. Mostafa, N. Ray Chaudhuri, Cryst. Growth Des. 7 (2007) 1365.
[100] J.T. Su, X. Xu, W.A. Goddard III, J. Phys. Chem. A 108 (2004) 10518.
[101] C. Pak, H.M. Lee, J.C. Kim, D. Kim, K.S. Kim, Struct. Chem. 16 (2005) 187.
[102] K.S. Kim, M. Dupuis, G.C. Lie, E. Clementi, Chem. Phys. Lett. 131 (1986) 451.
[103] B.J. Mhin, H.S. Kim, H.S. Kim, C.W. Yoon, K.S. Kim, Chem. Phys. Lett. 176 (1991) 41.
[104] J. Kim, K.S. Kim, J. Chem. Phys. 109 (1998) 5886.
[105] H.M. Lee, S.B. Suh, J.Y. Lee, P. Tarakeshwar, K.S. Kim, J. Chem. Phys. 112 (2000) 9759.
[106] K. Liu, M.G. Brown, C. Carter, R.J. Saykally, J.K. Gregory, D.C. Clary, Nature 381 (1996) 501.
[107] K. Nauta, R.E. Miller, Science 287 (2000) 293.
[108] U. Buck, I. Ettischer, M. Melzer, V. Buch, J. Sadlej, Phys. Rev. Lett. 80 (1998) 2578.
[109] C.J. Gruenloh, J.R. Carney, C.A. Arrington, T.S. Zwier, S.Y. Fredericks, K.D. Jordan, Science 276 (1997) 1678.
[110] B. Dey, S.R. Choudhury, P. Gamez, A.V. Vargiu, A. Robertazzi, C.-Y. Chen, H.M. Lee, A.D. Jana, S. Mukhopadhyay, J. Phys. Chem. A 113 (2009) 8626.
[111] G.R. Desiraju, J. Chem. Soc., Chem. Commun. (1991) 426.
[112] A.L. Gillon, N. Feeder, R.J. Davey, R. Storey, Cryst. Growth Des. 3 (2003) 663.